Optical Properties of a CH-type Focusing Lens

J. DiMarco, M. Tartaglia, I. Terechkine

I. Introduction

Requirements for the alignment accuracy for focusing lenses of HINS linac were introduced in the presentation of B. Mustapha, P. Ostroumov, and V. Aseev to HINS R&D meeting on Nov. 16, 2006 [1]. According to their model, in the CH section of the linac, the displacement of each end of a solenoid-based focusing lens (introduced in terms of its effective parameters: B_{eff} and L_{eff}) must be within ±0.15 mm of beam axis if no correctors are used, and less than ±0.3 mm if dipole correctors and beam position monitors with better than 10 μm sensitivity are employed.

The optimal placement of a focusing lens in a beam-line is on its optical axis, which does not always coincide with the mechanical (geometric) or magnetic axis. For example, Fig. 1 shows the mechanical offset of the magnet beam pipe center (a) and of the magnet yoke (b) from the magnetic axis (as found using a moving Single Stretched Wire (SSW) technique [2]) of a prototype lens.

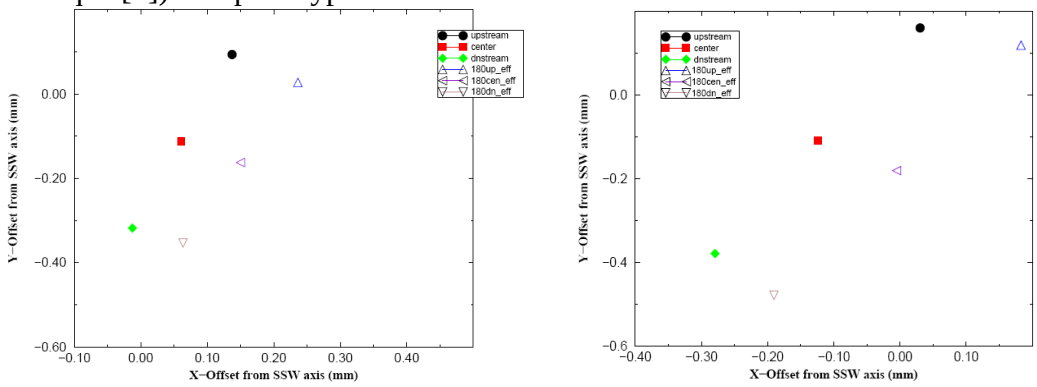

a) b)

Fig. 1. Offset of a beam pipe center (a) and a magnet yoke center (b) from the magnetic axis of a focusing solenoid.

The symbols in the figure show the X/Y transverse coordinates of the mechanical center and ends (‘upstream, ‘center’, ‘dnstream’) of the magnet relative to the magnetic axis (defined as (0,0)). The two sets of measurements correspond to two set-ups that have the magnet flipped 180º end-for-end to check for consistency. The relative shift of the mechanical and magnetic axis is ~0.3 mm (with precision of the measurements of the order of 50 μm) and is not parallel, but rather has angular (yaw and pitch) components. The results of these measurements indicate that if a certain degree of precision in focusing element positioning is needed, the axis must be found by making special measurements, e.g. as it was done in [3], where the magnetic axis of each lens was found using Hall probes, rather than relying on mechanics.

In addition, during cool down to cryogenic temperatures, the solenoid’s axis is going to shift. The shift pattern is complicated by mechanical connections of the lens: to the cryogenic supply line, current lead feed-through, and vacuum pipe. The scale of this shift is also expected on the level of half a millimeter. An attempt to understand the movement pattern in the prototype CH-type lens was made [4] using the SSW measurement system.

Graphs in Fig. 2 show migration of the magnetic axis in the horizontal and the vertical planes.

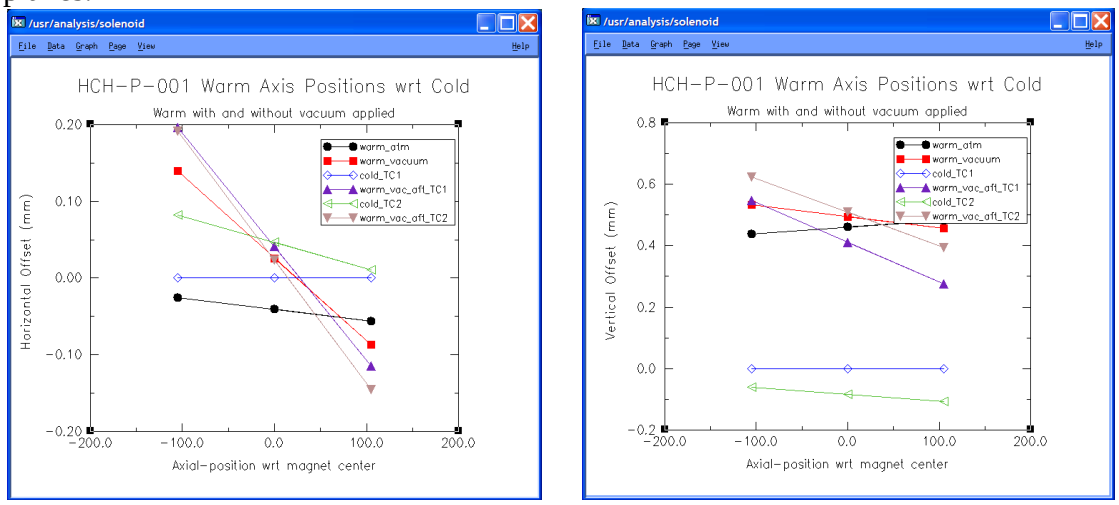

Fig. 2. Migration of the magnetic axis of a prototype CH-type focusing lens at different stages of the cool down.

Although this method provides valuable information about relative movement of the magnetic axis of a focusing lens, it remains unknown to what extent the information found by minimization of voltage induced on a wire moving in the magnetic field can be used to understand where the position of the lens optical axis is. ***We will define "optical axis" to be a line with the following property: the lens does not deflect a sample charged particle directed along this line.***

The goal of this study is to understand the limits of using the stretched wire technique for the purpose of solenoid-based lens alignment by using computational means. For this purpose, the magnetic axis position will be found using a numerical analog to the stretched wire technique and sample particle tracking will be used to find the optical axis. Properties of an ideal lens (built in accordance with the production drawings) will be studied first to verify the used approach; after that, a non-ideal lens will be studied. The initial beam energy of 2.5 MeV ($\beta = 0.073$) was chosen, corresponding to the input energy in the MEBT and CH section of the HINS linac. Parameters of the lens in the model correspond to the production CH-type lens [5]. These include the presence of bucking coils in the ends to dampen the extent of stray fields. Magnetic field distribution along the axis of this lens is shown in Fig. 3.

At 200 A, the squared field integral along the length of the lens is **2.038** T^2-m. The expected focusing length of a "thin" lens with this value of focusing strength is about 102 mm (e.g., see [6]). Because this focusing length is comparable with the length of our CH-type lens (~100 mm), we can expect some deviation from this value for the actual focusing length. The field integral at 200 A is **0.4725** T-m.

The coordinate system used in this note is as follows: the beam propagates along the X-axis (this definition of axial direction is chosen to match the computational code), with Y-axis horizontal, and Z-axis vertical (as indicated in Figure 4).

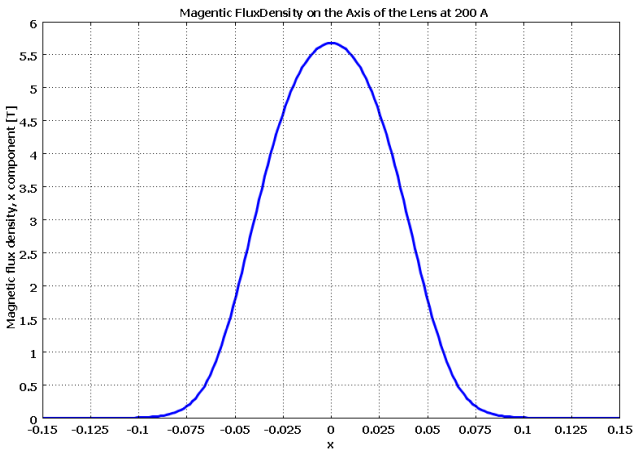

Fig. 3. Magnetic field profile in the CH-type lens at 200 A.

II. Optical properties of ideal CH-type focusing lens

II.A Basic optical properties

In this note, we will call an optical lens "ideal" if it is fabricated exactly as production drawings request (no deviations in any dimension). When calling a lens "perfect", we mean a lens without any aberrations. So the ideal lens is not always perfect, but rather it is always imperfect.

To understand how the lens behaves, sample particles with different initial conditions will be tracked. Each trace starts at the point X = X0, Y = Y0, and Z = Z0 and initially moves parallel to the X-axis. Let's choose X0 = -150 mm, Y0 = 0 and Z0 = 5 mm, 10 mm, and 15 mm. Modeling geometry is shown in Fig. 4 with the sample trajectories shown respectively in blue, green, and red.

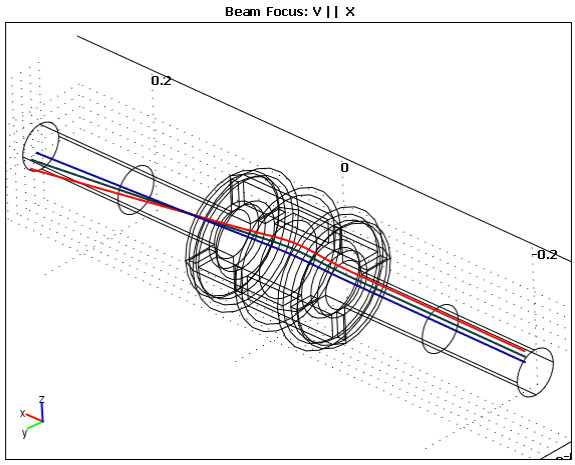

Fig. 4. Modeling geometry with three sample traces: Z0 = 5 mm, 10 mm, and 15 mm.

Fig. 5 shows projections of these three sample trajectories on the Y-Z plane. All three sample trajectories come close to the geometric axis (i.e. at some point they cross Y=0,

Z=0 and continue in a straight line); we also see the rotation of the beam trajectories around the X-axis.

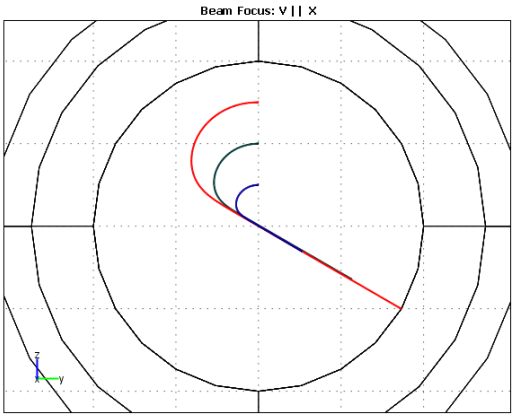

Fig. 5. Projection of the beam trajectories on the Y-Z plane.

To further study the trajectories with initial offset, Fig. 6 shows the same input beams as seen in the X-R plane (R= $\sqrt{Y^2 + Z^2}$) in the vicinity of the focal plane. All the trajectories are initially parallel to the geometric axis with the starting points distributed evenly around it at distances R0 = 0.15 mm, 5 mm, and 10 mm.

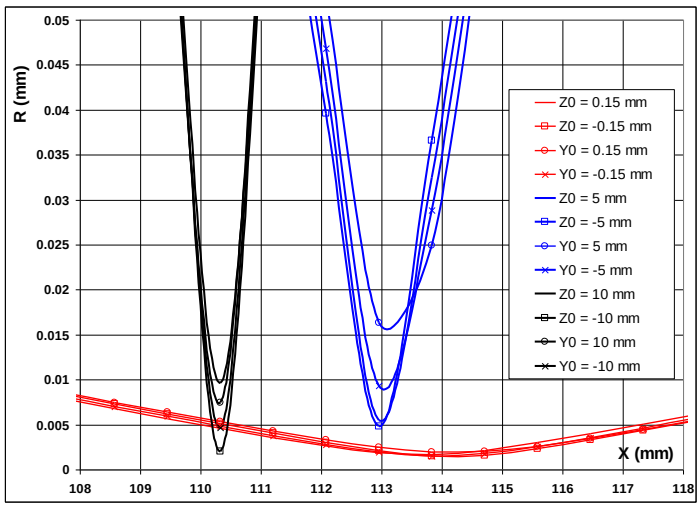

Fig. 6. Sample beam trajectory results near the focus plane (variations in R0 for a given starting distance can be attributed to numerical noise from the grid size used in this early study).

For a perfect (thin) lens the trajectories must touch the axis, i.e. reach R=0, at X=102 mm. In the ideal lens case, there are some aberrations: the focal length decreases as the starting distance from the center increases, and is always greater than the perfect thin lens case (as anticipated in section I).

The variations of focal plane distance seen in Fig. 6 bear resemblance to the distortion effects caused by spherical aberration. A sketch demonstrating such distortion in an

optical lens is shown in Fig. 7 (also see ref. [8]). The radial size of the aberration defines the quality of any lens and depends on many details. In Fig. 6, for trajectories closer to the axis, the size of the aberration can be just several microns; for the traces farther from the center, this distance is 10 to 15 μm.

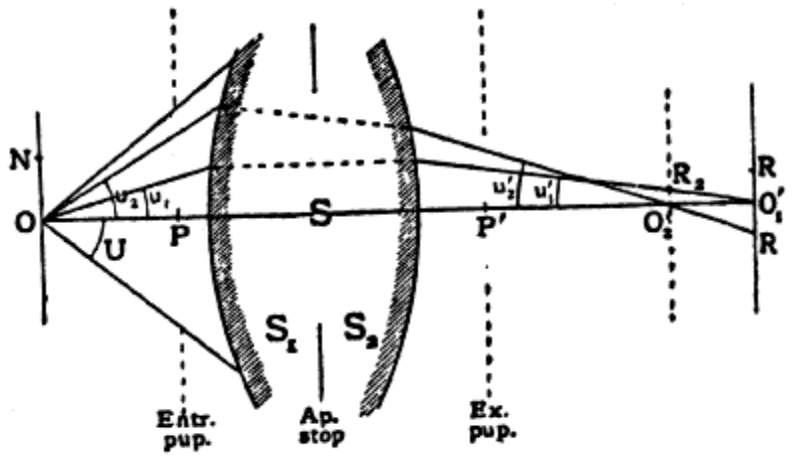

Fig. 7. Spherical aberration in the optical lens

The focusing length is close to what can be expected based on the distribution of the magnetic field along the axis in Fig. 3, as given by the equation

$$f = \frac{8 \cdot \frac{m}{q} \cdot U}{\int_{-\infty}^{+\infty} B_X^2 \, dX} \quad , \qquad /1/$$

where SI units are used, except for U, which is in eV.

The rotation of the trajectories around the X-axis seen in Fig. 4 and Fig. 5 can also be evaluated based on the distribution of the magnetic field B(x) along the X-axis. Having in mind specifics of the particle motion in the longitudinal magnetic field of a solenoid (see [6]), the angular frequency, ω, of the rotation around the geometric axis is

$$\omega = (e \cdot B)/(2m) \qquad /2/$$

Then, for a short lens, the angle change, dφ, is given by

$$d\varphi = (\omega/\beta c) \cdot dx \qquad /3/$$

After integrating from the starting point X0 (where B = 0) to X (which is any place along the axis) we have:

$$\varphi(X) = \frac{e}{2 \cdot m \cdot \beta \cdot c} \int_{X0}^{X} B(x) \cdot dx \qquad /4/$$

The rotation angle is defined by the magnetic field integral along the axis. Fig. 8 shows how this rotation angle changes along the axis of the lens for the three sample beams in Fig. 5. Also shown in Fig. 8 is the ideal rotation angle as defined by equation /4/.

To conclude this part of the study, we can say that ***the beam optics computational analysis gives trustable results that compare well with theoretical predictions***. So, we can use this tool to further investigate optical properties of the lens.

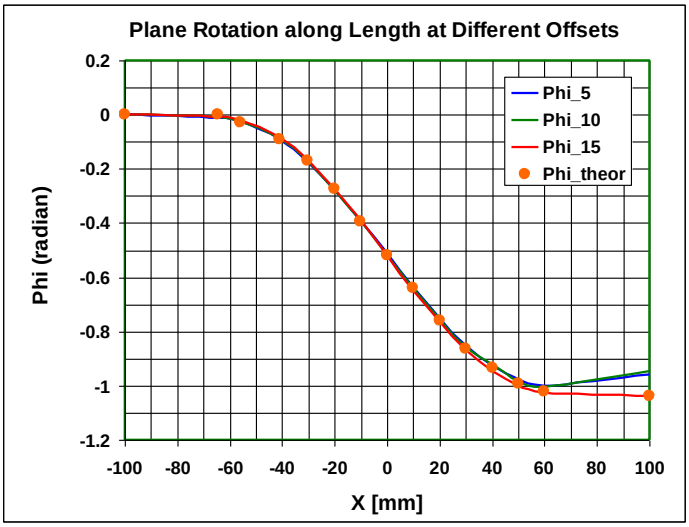

Fig. 8. The rotation experienced by the beam cross-section as it traverses the length of the lens.

II.B Transfer Matrix

As mentioned earlier, the beam modeling software usually uses effective parameters of optical elements and transfer matrices based on these parameters. In the case of a solenoid-based lens, the effective parameters are effective magnetic field and effective length defined using the following equations:

$$B_{eff}^2 \cdot L_{eff} = \int_{-\infty}^{+\infty} B_X^2 \, dX \quad \text{and} \quad B_{eff} \cdot L_{eff} = \int_{-\infty}^{+\infty} B_X \, dX \qquad /5/$$

In the case of a CH lens, at 200 A, $B_{eff}^2 \cdot L_{eff} = 2.038$ T^2·m, and $B_{eff} \cdot L_{eff} = 0.4725$ T·m. It is easy then to find B_{eff} and L_{eff}: $B_{eff} \approx 4.31$ T and $L_{eff} \approx 0.11$ m.

By using the effective values for the magnetic field and the length, in the first order approximation, one gets optical properties of a model lens identical to those of a "real" lens. The transfer matrix for a solenoid-based lens has the following structure [7]:

$$\mathrm{R} = \begin{vmatrix} C^2 & \frac{SC}{K} & SC & \frac{S^2}{K} \\ -KSC & C^2 & -KS^2 & SC \\ -SC & -\frac{S^2}{K} & C^2 & \frac{SC}{K} \\ KS^2 & -SC & -KSC & C^2 \end{vmatrix} \qquad /6/$$

Here K = B_{eff} / [2(p/q)], where (p/q) is particle momentum expressed in eV/c units: $\frac{p}{q} = \sqrt{2\left(\frac{m}{q}\right)\cdot\left(\frac{U}{q}\right)}$, where U is kinetic energy in electron-volts (eV), m is the proton mass ($1.67\cdot10^{-27}$ kg), and q is the proton charge ($1.6\cdot10^{-19}$ Coulomb). Using the known B_{eff} , L_{eff}, and U results in K = -9.4333. Also, in the matrix, S = sin(KL) and C = cos(KL), with L = L_{eff}. Because coefficients K and S are field-dependent, signs of the coefficients in the matrix are defined by the direction of the magnetic field. With this in mind, the transfer matrix R of a CH-type lens at 2.5 MeV becomes

$$R = \begin{vmatrix} 0.2617 & 0.0466 & -0.4396 & -0.07825 \\ -4.1469 & 0.2617 & 6.9636 & -0.4396 \\ 0.4396 & 0.07825 & 0.2617 & 0.0466 \\ -6.9636 & 0.4396 & -4.1469 & 0.2617 \end{vmatrix} \qquad /7/$$

Quantity "–KL", which is the argument of the sine functions in /6/, defines the angle of the polarization plane rotation after the lens. In our case it is -1.034 radian, which is close to the value $\Delta\varphi$ = -1.04 radian found earlier by other means.

Knowing initial position and transverse velocity of the sample particle at X = -L_{eff}/2, we can find y, y', z, and z' at X = +L_{eff}/2 by using the transfer matrix /7/. Having in mind that the field of the real solenoid protrudes beyond the effective length, we should not expect perfect agreement. For one of the sample traces, we have the initial vector of coordinates and angles at the entrance to the lens (X = -L_{eff}/2) (all coordinates are in mm and the angles are in radians):

$$V0 = \begin{pmatrix} y0 \\ y0' \\ z0 \\ z0' \end{pmatrix} = \begin{pmatrix} -0.146 \\ -0.01477 \\ 4.996 \\ -0.0006 \end{pmatrix}$$

Applying the matrix transformation to this vector, we calculate the coordinates and the angles at the exit of the lens (X = +L_{eff}/2):

$$V1 = \begin{pmatrix} y1 \\ y1' \\ z1 \\ z1' \end{pmatrix} = \begin{pmatrix} -2.9 \\ 0.032 \\ 0.06 \\ -0.026 \end{pmatrix}$$

When using a sample trace, the initial vector V0 at X = -L_{eff}/2 transforms into the vector V1_tr at X = +L_{eff}/2 :

$$V1\_tr = \begin{pmatrix} y1 \\ y1' \\ z1 \\ z1' \end{pmatrix} = \begin{pmatrix} -2.5 \\ 0.032 \\ 0.13 \\ -0.025 \end{pmatrix}$$

This vector compares well (although not in the perfect agreement) with that obtained by the matrix transformation.

III. Axis determination of an ideal CH-type focusing lens

III.A Sample particle tracing method applied to the ideal lens

As was stated in the introduction, by analogy with the optical elements, the main optical axis is a straight line along which the ray (light, or particle) passes without deviation. For a perfectly axial-symmetric (ideal) lens this is the axis of geometric symmetry. An optical ray passing through the center, but not along the geometric axis of the lens, will deviate a bit from a straight line, as happens in a real optical lens. In preparation for dealing with a non-ideal lens, where the axial symmetry is not perfect, we can try to find the optical axis by looking at the mean square deviation of a sample particle trajectory from a straight line that passes through the emission point and the center of the solenoid-based lens. One possible search algorithm is the following:

1. The emission point is chosen and sample particle is sent towards the center of the lens. The reference line is defined by the particle's initial velocity and position;
2. Deviation of the particle trajectory (calculated using the computational model) from this reference line is determined;
3. Adjustment is made of the particle initial conditions (position and velocity);
4. Iterate steps 2-3 until the needed degree of accuracy is achieved.

To check how this procedure works in the case of an ideal lens, let's choose the initial position of the sample particle in the XZ plane, near the left focal plane (X0 = -110 mm). The initial transverse component of the velocity will be

$$V0z = \beta \cdot c \cdot Z0/X0.$$

The squared distance between the computed trace trajectory (X, Y, Z) and the line $Z = \frac{Z0}{X0} \cdot X$ is

$$D^2 = (Z - X*Z0/X0)^2 + Y^2$$

If Z0 = -1 mm, V0z = 0.073*2.99793e8*1/110 = 2.0843e5 m/s.

Next we will implement the algorithm described earlier and step through a range of particle trajectory conditions :

a) Without changing V0z, make Z0 = -0.5 mm;
b) Replace V0z by V0z/2 to send the previous line through the center;
c) Make V0z = 0;
d) Make Z0 = 0; leave V0z = 0;
e) Leave Z0 = 0; restore V0z to the previous value of 104215 m/s.

Values of the integrated squared distance $\int D^2 dx$ are summarized in the Table 1:

Table 1

Conditions	Initial	a)	b)	c)	d)	e)
Z0 [mm]	-1	-0.5	-0.5	-0.5	0	0
V0z [m/s]	2.0843e5	2.0843e5	1.04215e5	0	0	1.04215e5
$\int D^2 dx$ [m^3]	**5.4e-07**	**2.9e-7**	**1.4e-7**	**1.7e-7**	**8.1e-9**	**6.6e-8**

As one would expect, the minimum value of the integral takes place when the trace starts on the axis (Z0 = 0) and is directed along the axis (V0z = 0). Because this value is about ten times smaller than the nearest one, the optical axis is easy to identify.

III.B Moving Stretched Wire method applied to the ideal lens

Now a moving wire (MW) technique can be applied to the ideal lens, with perfect geometry, to check how sensitive this method is and to evaluate the noise level. When a wire is moved in the magnetic field (with the return wire of the loop held fixed), a voltage is induced that is defined by the flux change rate:

$$U = d\Phi/dt.$$

In turn, the flux change rate depends on the velocity of the wire and the magnetic flux density component perpendicular to the plane of the movement, Bn:

$$d\Phi/dt = \int Bn \cdot v \cdot dx$$

In the case of the parallel wire movement (both ends of the wire moving co-directionally), the velocity is constant, and

$$U \sim \int Bn \cdot dx.$$

If the movement is in opposite directions at the ends of the lens (counter-directional motion), the wire velocity is proportional to the distance from the point that does not move (the center), and to a good approximation

$$U \sim \int x \cdot Bn \cdot dx.$$

So, we can model the expected relative voltage (and the absolute value also) by taking appropriate integrals along any line within the lens aperture. Sample results obtained by using this technique in the case of the ideal lens are summarized in Table 2. The integrals are taken along the axis of the lens: from X = -0.1 m to X = +0.1 m.

Table 2

	Z1 = 0; Z2 = 0	Z1 = 1; Z2 = 1	Z1 = 1; Z2 = -1
$\int Bz \cdot dx$	3e-3	6e-3	**2.3**
$\int x \cdot Bz \cdot dx$	6e-5	**0.24**	7.5e-5
$\int By \cdot dx$	3.7e-3	2e-3	4e-3
$\int x \cdot By \cdot dx$	6e-5	1.5e-4	2e-6

To check consistency, simple cases can be examined. When the integration line is along the axis, zero signal is expected. If the endpoints of the line of integration are Z1 = Z2 = 1 mm, counter-directional wire motion in the XY plane results in a pronounced signal $U = \int x \cdot Bz \cdot dx$, which is in accordance with the expected behavior for a transverse offset. If the integration line is from Z1=1 mm to Z2 = -1 mm (crossing the axis at X = 0), co-directional Y-movement results in the angular misalignment signal $U = \int Bz \cdot dx$. Here we measure U in arbitrary units (a.u), but it is quite straightforward to switch to volts.

Some numerical noise exists due to the finite size of the mesh. However, by properly choosing the mesh size, the numerical noise is much lower than the useful "signal", which is proportional to the wire movement amplitude. If ~0.004 a.u. noise level is

acceptable (inferred from the ideal case Z1 = Z2 = 0, where theoretically all the signals must be zero), we can conclude that we can resolve the axis of the lens with an accuracy of about 20 μm.

III.C Vibrating Wire method applied to the ideal lens

The vibrating wire (VW) technique involves applying an AC current, tuned to a resonant frequency of the wire, as it is stretched through the solenoid lens. If the wire is not on the lens axis, a transverse force is felt by the wire. The wire displacement is measured and a voltage proportional to the displacement is generated. The transverse displacement can be described as a superposition of sinusoidal standing waves with ends constrained at X1, X2. The lowest frequency (half-wave) mode will result in the wire displacement $y = y0*\cos(\pi \cdot x/2X0)$, where the maximum deflection is at X= 0 (i.e. the axial center of the lens). Displacement for the next (one-wave) mode will have a zero in the center of the solenoid: $y = y0*\sin(\pi \cdot x/X0)$. An attempt to find the magnetic axis using these two modes of motion leads to evaluation of the integrals:

$$\int \cos(\pi \cdot x/2X0) \cdot Bz \cdot dx \quad \text{and} \quad \int \sin(\pi \cdot x/X0) \cdot Bz \cdot dx.$$

In an analogous way to the MW technique of III.B, finding wire positions which minimize the voltage signal from wire displacement allows determination of the lens magnetic axis. The results of the VW measurement applied to the case of an ideal solenoid lens yield results that are consistent with the MW technique and the ideal axis to within the uncertainty caused by the finite mesh size (20 μm).

VW measurements over a spectrum of resonant frequencies may also yield information about the position of the local magnetic center, i.e. the YZ coordinates along X where the transverse component of magnetic field is zero.

IV. Axis determination of a non-ideal CH-type focusing lens

Now we can switch to a non-ideal case. Let's move one of the bucking coils of the ideal lens (the side where a sample particle enters the lens) vertically by 1 mm, and try to locate the lens magnetic axis by applying the single stretched wire technique. Because we have the bucking coil shifted vertically, we should expect the new effective magnetic axis also to be in the vertical plane. After the position of the magnetic axis is found, beam tracking will be used to check whether the found position functions as an optical axis of the lens. Both the moving wire (MW) and a vibrating wire (VW) methods will be used. In both cases, the wire ends are fixed at the points X1 = -100 mm and X2 = 100 mm.

IV.A Moving Wire magnetic axis of a non-ideal lens

Table 3 summarizes the magnetic axis search results when the **MW** method is used for various initial positions of the wire. The minimum integrated signal is observed if the wire is stretched along the line from point (-100 mm, 0, 0.405 mm) to the point (100 mm, 0, -0.185 mm).

Table 3

	$\int Bz \cdot dx$	$\int x \cdot Bz \cdot dx$
Z1 = 0 Z2 = 0	7.0e-1	-2.6e-2
Z1 = 0.5 mm Z2 = 0.5 mm	7.0e-1	9.2e-2
Z1 = 0.5 mm Z2 = 0	0.11	3.3e-2
Z1 = 0.3 mm Z2 = -0.2 mm	0.11	-1.4e-2
Z1 = 0.2 mm Z2 = -0.3 mm	0.11	-3.7e-2
Z1 = 0.35 mm Z2 = -0.15 mm	0.11	-2.1e-3
Z1 = 0.4 mm Z2 = -0.2 mm	-0.011	-2.1e-3
Z1 = 0.395 mm Z2 = -0.195 mm	8.8e-4	-2.1e-3
Z1 = 0.397 mm Z2 = -0.197 mm	8.8e-4	-1.6e-3
Z1 = 0.405 mm Z2 = -0.185 mm	**5.3e-4**	**2.7e-4**

IV.B Vibrating Wire magnetic axis of a non-ideal lens

As was done for the MW case, the Z-position at X = ±X0 is changed to find the minimum value of the integrals. The results of the search are summarized in Table 4.

Table 4

	$\int \cos(\pi \cdot x/2X0) \cdot Bz \cdot dx$	$\int \sin(\pi \cdot x/X0) \cdot Bz \cdot dx$
Z1 = 0 Z2 = 0	0.58	-0.59
Z1 = 0.5 mm Z2 = 0.5 mm	0.58	1.76
Z1 = 0.5 mm Z2 = -0.2 mm	$2.6*10^{-3}$	0.116
Z1 = 0.47 mm Z2 = -0.23 mm	$2.8*10^{-3}$	$-2.5*10^{-2}$
Z1 = 0.475 mm Z2 = -0.225 mm	$2.8*10^{-3}$	$-1.6*10^{-3}$
Z1 = 0.472 mm Z2 = -0.222 mm	$7.4*10^{-3}$	$-2.0*10^{-3}$
Z1 = 0.477 mm Z2 = -0.227 mm	$\mathbf{-4.6*10^{-4}}$	$\mathbf{-1.6*10^{-3}}$

In this case, the effective magnetic axis is going through the points (-100, 0, 0.477) and (100, 0, -0.227), which differs from what was found by using the MW method. This difference is due to the fact that the moving stretched wire, if not coming along the axis of an ideal lens, is sensitive to the axial component of the magnetic field inside the lens, which is orders of magnitude stronger than the transverse component under bucking coils. So, different wire movement patterns result in different (although not dramatically different) integrated displacement signal.

Such differences have been seen in recent studies with the SSW system to determine the magnetic axis using, and comparing, both MW and VW techniques. These have been made with an available SS1 pre-production solenoid lens (which differs somewhat from the CH lens) in which individual coil axes can be measured and compared to the series-connected lens, albeit at room temperature. The quantitative analysis of these measurements is still under way.

IV.C MW magnetic axis position dependence on size of BC displacement

The graph in Fig. 9 expands on the result of the magnetic axis search using the MW method (section IV.A) for a range of displacements of the BC. Note that for this study, the coordinates of the front (Z1) and the rear (Z2) positions of the magnetic axis are at X1 = -200 mm and X2 = +200 mm, where the magnetic field is practically zero. Note that the measured axis shift is approximately linear with bucking coil shift.

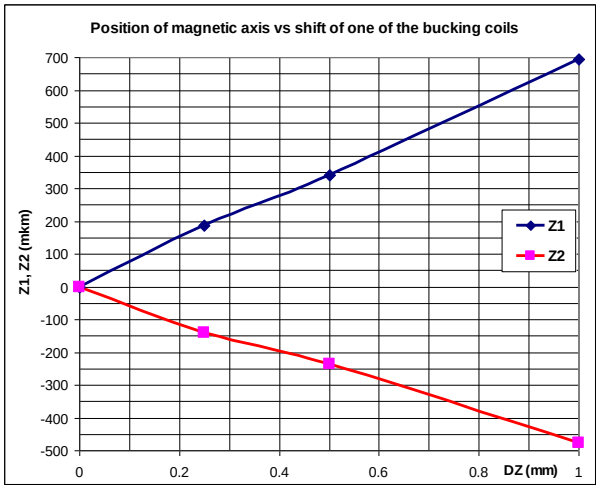

Fig. 9. The front (Z1) and the rear (Z2) coordinates measured by MW to be the magnetic axis depending on the front BC shift (DZ) value. X1 = -200 mm, X2 = 200 mm.

In fact, the tolerances for solenoid fabrication allow a maximum expected shift in the BC position of about 0.25 mm with respect to the main coil axis. Then, from Fig. 9, we can expect in such a case that the magnetic axis would be a line passing through the points (-200, 0, 0.2) and (200, 0, -0.15). This translates into vertical offsets of 0.05 mm and -0.04 mm at the ends of the solenoid, which are at X= -50 mm and X= +50 mm, respectively. These would be within the tolerances specified for solenoid alignment.

IV.D Particle tracking using magnetic axis results in a non-ideal lens

Now we can use particle tracking to see if a trace initiated along the magnetic axis found by MW corresponds to an optical axis (i.e., whether the trace remains un-deviated as it passes through the non-ideal lens). Using the result of section IV.A, the sample trace starts at the (focal plane) point (X,Y,Z) = (-105, 0, 0.420) and is directed along the stretched wire (starting angle of -0.00295), so that the projection of this direction passes through the point (105, 0, -0.205). The results are presented in Fig. 10, which shows a projection of the trajectory on the YZ plane. We find that at X = +150 mm the trajectory deflects by ~1.4 mm from the line determined by the stretched wire. As one can see, the trajectory does not cross the plane Z = 0; so, by definition it does not correspond to the optical axis.

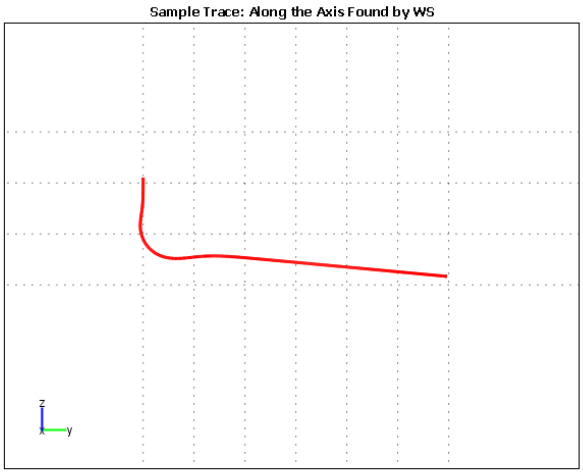

Fig. 10. Projection of the trajectory on the YZ plane for the trace directed along the axis found by the MW scanning technique. Grid covers the area where Y>0 and Z>0; the distance between the grid lines is 0.2 mm.

We can explore how this result depends on the initial size of the BC shift. For each value of the BC shift, Z0, the corresponding magnetic axis is found. We send a sample particle along this MW magnetic axis and measure the distance from the particle trajectory to the magnetic axis and to the geometric axis of the main coil (as measured at X=+260 mm). These data are plotted in Fig. 11 as a function of different values of the shift in upstream BC. For the 0.25 mm BC displacement, the distance from the trace to each axis is ~0.35 mm.

From the data in this section, it is clear that although the position of the magnetic axis is known, we cannot rely on this information to find the optical axis. The problem with this approach to locating the optical axis is that the area within the lens that the stretched wire samples is different from that which a sample particle travels. The stretched wire technique identifies the line along which the inductive voltage due to wire movement is minimal. A sample particle does not move along this straight line, but rather along a 3-D trajectory with the curvature depending on the particle location and velocity vector. We should not expect the solution determined from sample particle trajectories to coincide with that determined from MW/VW technique.

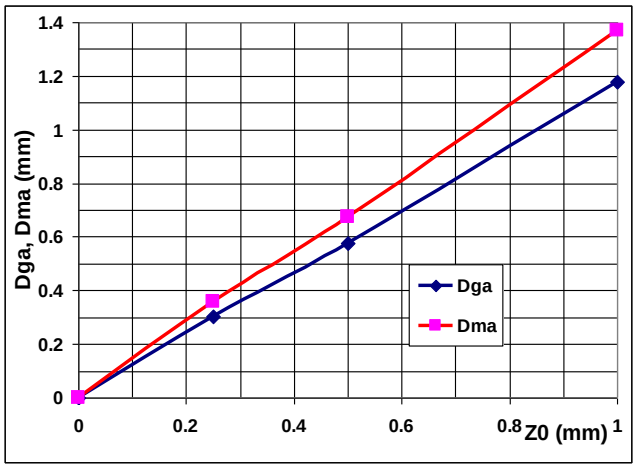

Fig. 11. The distance of a particle from its initial trajectory line (and its distance from the geometric axis of the main coil) is shown vs. BC offset. The MW magnetic axis is used as the initial trajectory line, with starting position at X1 = -200 mm and evaluated at X2 = 260 mm. Distance to geometric axis is shown as Dga, and to magnetic axis as Dma.

IV.E Finding a sample optical axis in a non-ideal lens

To see if an optical axis exists for this non-ideal solenoid, we will change the initial position and transverse velocity of a sample particle to obtain a trajectory that is close to a straight line; i.e. a projection of the starting point along the initial velocity. This is conveniently achieved while watching the projection of the trajectory on the YZ plane (as done in Fig. 10). One of the close candidates for this axis is shown in Fig. 12. The initial position of the beam here is X0 = -105 mm, Y0 = -0.035 mm, and Z0 = -0.08 mm. The initial transverse velocities were: V0y = 10000 m/s and V0z = 25000 m/s.

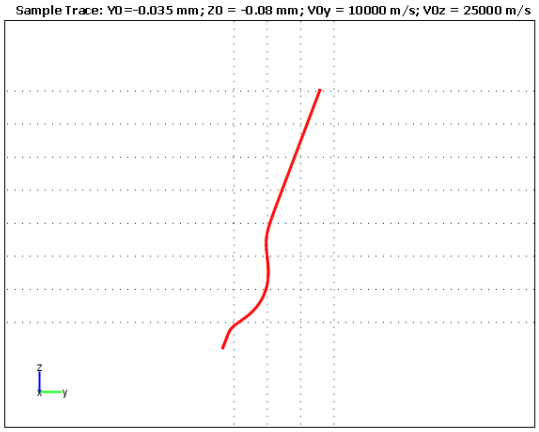

Fig. 12. Projection of the trajectory on the YZ plane for the trace directed along the axis found by the beam tracing. The distance between the grid lines is 0.1 mm.

The sample trajectory almost hits the main geometric axis (that of the main coil of the lens) coming just ~3 μm off it (though not at X=0) (see Fig. 13). The maximum deviation of the trace from the initial direction is ~100 μm. So, we can conclude that this line is

quite close to what we would call the “effective optical axis” of this non-ideal lens. Nevertheless, the initial position and the velocity of the sample particle is quite different from what we would expect based on the magnetic axis position found earlier. Such an axis is not practically useful, since it is not intuitive how to find it from measurements, and it depends on the particle having a particular trajectory.

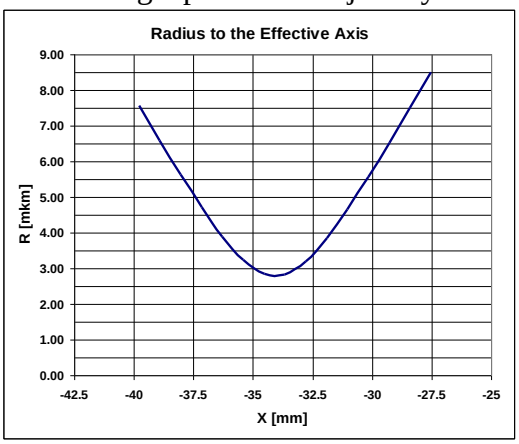

Fig. 13. Distance (in microns) between the effective and the main axis for a set of initial conditions which find an optical axis for a non-ideal solenoid.

IV.F Particle tracking using data from local magnetic axis in a non-ideal lens

By the analogy with an optical lens, we can expect that there are many other candidates for the optical axis of the lens. Although no perfect optical axis can be found for a non-ideal lens, we are interested to find an axis close to that found by the MW/VW method.

First, let's locate a line inside the lens that is passing through the points where the radial component of the magnetic field is zero. One way of finding this line in the lens would be to make Hall probe scans. This line, as determined from magnetic modeling of the lens having a 1mm bucking coil shift on one end, is shown in Fig. 14.

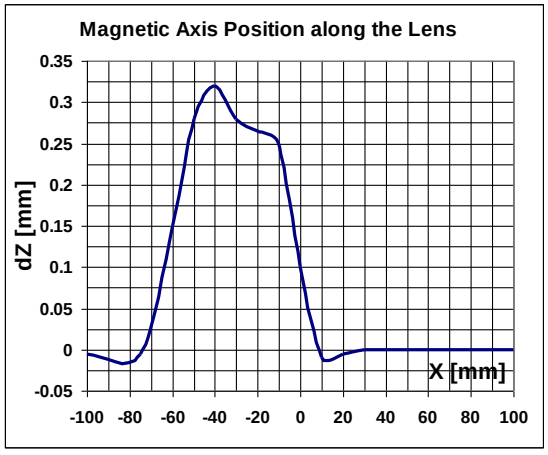

Fig. 14. Position of points with zero radial field in the non-ideal lens.

The maximum deflection of this line from the axis of the main coil is ~0.3 mm. (Note that the expected shift of lens elements due to assembly accuracy is better than 0.25 mm,

so this implies that the magnetic axis shift should not exceed ±0.1 mm (at each end of the lens) during production). Because the second bucking coil was not shifted, we will start looking for a new effective axis position above the main axis.

Table 7 summarizes results of several modeling trials with different initial conditions consistent with the local magnetic axis shift of Fig. 14. The quantities to watch were the maximum deflections from the main axis (Y, Z) and from the projected optical line (D) at X = 150 mm along the initial beam direction.

Table 7

Y0, Z0 [mm]	Vy, Vz [m/s]	Y @ X = 0.15 m	Z @ X = 0.15 m	D @ X = 0.15 m
0, 0.41	0, -64561	1.2	0.03	1.4
0.1, 0.4	20000, -5000	0.87	0.22	0.45
0.01, 0.3	9000, 500	0.76	0.34	0.6
0, 0.3	9000, 0	0.77	0.35	0.62
0, 0.3	0, 0	0.74	0.3	0.74
0, 0.25	0, 0	0.69	0.34	0.69
0, 0.2	0, 0	0.63	0.37	0.65
0, 0.15	0, 0	0.58	0.4	0.63
0, 0.1	0, 0	0.52	0.43	0.62
0, 0.05	0, 0	0.47	0.46	0.62
0, 0	0, 0	0.42	0.5	0.65

The minimum distance from the trace to the optical projection line (D) could not be made less than ~0.5 mm at X=150mm. Having only this information, no clear conclusion for optical axis can be made; the initial position with Z0 = 0.05 mm is, although close to optimal, not much better than the others, and still has large deviation. The graph in Fig. 15 visualizes the data of Table 7 for the subset which has zero transverse velocities and starting point in the XZ plane (i.e. where Y0=0).

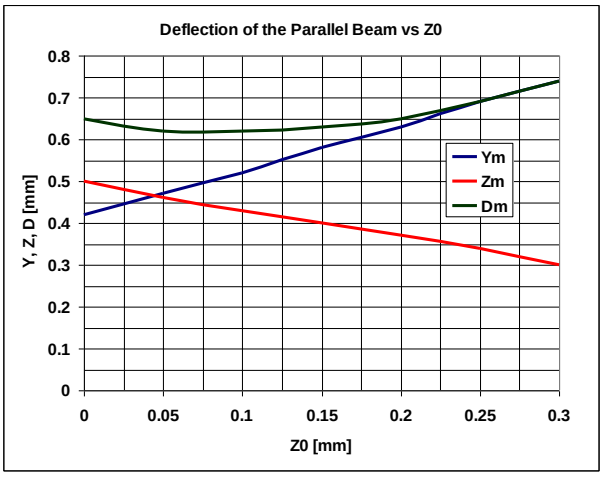

Fig. 15. Tracking summary results at X = +150 mm where initial trace direction is parallel to the main coil axis (Vy = 0, Vz = 0), and the vertical start position varies from Z0 = 0 to Z0 = 0.3 mm as suggested by local magnetic axis shifts.

IV.G Particle tracking using data from the magnetic axis of the Main Coil in a non-ideal lens

From the previous section, the indication is that the main coil axis may serve as a better guide to alignment of a non-ideal lens than the wire measurements of the magnetic axis, which is skewed by displaced bucking coils.

If we know the location of the MC magnetic axis (which corresponds to the MC geometric axis, assuming that the main coil is 'ideal'), we can use this as a reference axis. In practice, this axis can be determined by applying a Fourier transformation method with the VW technique, or by making Hall probe scans, as in [3], or by employing a pulsed current method as in [9].

The results of trajectory deviation from the main coil axis are shown in Fig. 16 as a function of the BC displacement. The distance from the trajectory to the reference axis, plotted as Dga, is significantly smaller than that found using the magnetic axis (Fig. 12, in section IV.D).

Since there are uncertainties in defining the position of the magnetic axis, whether it be that of the main coil, or that found by MW, etc., one can consider using an average of several different methods in hopes of reducing the overall uncertainty. The second curve in Fig. 16 (Dav) shows the distance to the main coil (i.e. geometric) axis in the case where the sample trace starts at the average between geometric and MW determined magnetic axes.

This analysis indicates that it would be useful to know the position of the geometric axis of the main coil. The alignment attempt using the magnetic axis of the MC seems to result in smaller particle deviation (by a factor of ~2) than using the axis of MC+BC. Both may be acceptable, however, depending on the actual tolerances required.

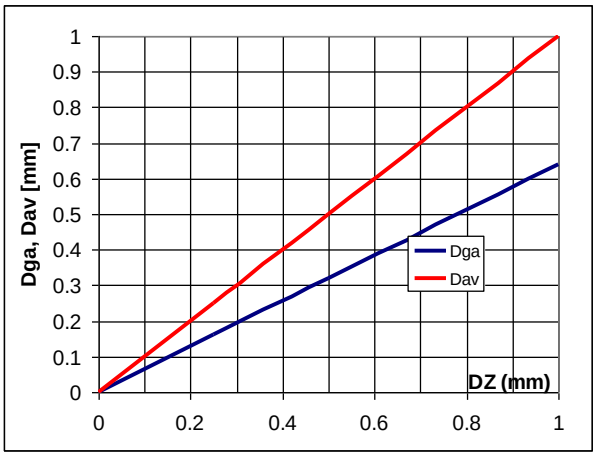

Fig. 16. Distance deviation from main coil geometric axis, evaluated at X=+260mm, as a function of the BC vertical displacement. The sample trace started on the magnetic (geometric) axis of the main coil (Dga), or between geometric axis and magnetic axis (Dma).

V. Comparison of aligned non-ideal lens with shifted ideal lens

To get a feeling of where we are in terms of the existing alignment requirements for lenses of HINS linac, let's compare beam distortions in the case of the non-ideal lens positioned using the geometric axis of the main coil with that in the case of a tilted or shifted ideal lens. The lens alignment analysis made in the early stage of the HINS linac development [1] provided a reference number for acceptable statistical uncertainty of the ideal lens positioning. If no correctors are used, a 0.15 mm amplitude of random displacement on both sides of the lens was considered acceptable. With the effective length of the lens ~100 mm, this corresponds to ~0.003 radian random tilt angle amplitude. Two families of sample particles will be used for this test. The particles of the first family start at X1 = -200 mm and go along a straight line parallel to the axis at the distance 0.15 mm from the axis. The particles of the second family also start at X1 = -200 mm and initially move along the straight lines parallel to the XZ plane, but with angle with respect to the XY plane of $\theta = 0.003$ radians. In both cases, we will record the distance from the initial direction line to the corresponding sample particle trajectory at X = 260 mm. Corresponding data are shown in Table 8.

Table 8

Y (mm)	0	0	0.15	-0.15	0	0	0	0	-0.6	0.6
Z (mm)	0.15	-0.15	0	0	-1.2	-0.6	0	0.6	0	0
Θ (rad)	0	0	0	0	0.003	0.003	0.003	0.003	0.003	0.003
Dg (mm)	0.3	0.3	0.3	0.3	1.4	0.7	1.4	2.4	1.2	2.2

The data in the table must be compared to that in Fig. 16 for the non-ideal lens. If we use the geometric axis of the main coil as a reference, the maximum statistical shift of the bucking coil must be on the level of ~0.5 mm to result in the sample particle deflection corresponding to the 0.15 mm parallel shift of an ideal lens (which showed D=0.3 mm). As mentioned previously, for the CH lenses, the maximum displacement of the bucking coil in the lens assembly should not exceed ±0.25 mm, so this should give trajectory displacements within those generated by the 0.15 mm parallel alignment tolerance.

The maximum bucking coil shift must be more than 2 mm (extrapolating past the data in Fig. 17) to result in the same sample particle deflection that happens when the ideal lens's tilt is ~3 mrad.

Obviously, the sensitivity of the optical system to the tilt is greater than that to the parallel displacement, and if a 3 mrad (±0.15 mm over the 100 mm distance) tilt is acceptable, the tolerances to the parallel shift can be relaxed. Conversely, if the angular tolerances should generate displacements consistent with those resulting from the parallel ones, the tilt tolerances should be much tighter. This may also require that the tolerances of mechanical alignment of the BC in the lens during fabrication be made smaller than the ±0.25 mm. This disparity in the requirements of parallel/angular displacements makes one wonder if the tolerances have been considered thoroughly.

In concluding this section, it is possible to say that the beam displacement effects generated by trying to align a non-ideal solenoid are of about the same magnitude as the misalignment tolerances specified for ideal lenses. These tolerances may need to be reformulated based on tracking studies such as this.

VI. Beam-based alignment

The most reliable way to align the lens is to use beam-based alignment. In this case, two pinholes can define a straight line along which the solenoid axis must be positioned. By moving the solenoid, position of the axis is adjusted so that the beam after the lens passes along the same line with the magnetic field on and off. By definition, this will define the optical axis of the lens.

It is, maybe, possible to use electrons for the alignment. In this case, we need to have the electron velocity close to that of ions. If the proton energy is 2.5 MeV, corresponding electron energy must be ~1362 V to have the same $\beta = 0.0729$. Magnetic field must be adjusted, so that the acceleration of the electrons in the lens is similar to that of the protons. This acceleration $a = e/m \cdot \beta c \cdot B$, so the magnetic field must be reduce by the factor $m_p/m_e = 1835$. If the initial effective magnetic field $B_{eff} = 23.5$ G. To get this field, the current in the CH-type lens must be set on the level of 200/1835 = 109 mA. The flux return must be demagnetized while doing this alignment, and the earth magnetic field must be shielded. Because the measurements must be made both in the warm and in the cold condition, strand magnetization can be a significant factor that complicates interpretation of the results if the strand becomes superconducting, so, superconducting strand temperature must be above the transition.

Because there will be beam position monitors (BPM) embedded in each lens, we can adjust position of the solenoids one by one after they are installed in the beam line. Position of BPM-s must be closely monitored during this adjustment, and corresponding algorithm must be developed.

Conclusions

Simulations have been made of ideal (perfectly constructed) and non-ideal (bucking coil displaced from main coil axis) CH solenoid lenses, to understand the relationships between optical axis measurements and behavior of particles traversing the lens. These studies included simulation of the Single Stretched Wire techniques, both Moving Wire (MW) and Vibrating Wire (VW), for finding the axis. Also, sample particle trajectories were simulated to find the best estimate of the optical axis – along which a moving particle is undeflected – and the relationship to the axis found by the wire approaches. BC shifts up to 1 mm were considered, although the maximum expected is about 0.25 mm, but the results are in general linear with this displacement. The following conclusions can be drawn from these studies:

1. With a 1 mm BC shift, the local magnetic center shift becomes as large as ~0.3 mm (i.e. position of zero radial field center varies as a function of axial position by 0.3mm – see section IV.E).

2. The magnetic axis found using MW technique (direction of zero average magnetic flux change with small transverse wire motions) reproduces the ideal lens optical axis to an accuracy of about 20 μm (III.B). However, it does not necessarily correspond to the optical axis of a non-ideal focusing lens. Rather a non-ideal lens does not have a well-defined optical axis, and actual particle trajectory through such a lens is generally complex and must be simulated.

3. Differences between moving and vibrating wire techniques can be reasonably explained by the lens being non-ideal. VW and MW techniques, which have different sensitivity to the field distribution, can differ measurably for a bucking coil at one end shifted by 1 mm. Further quantitative analysis of these differences is under way from measurements made on the SS1 pre-production lens, in which it was possible to separately determine the individual and combined lens axes.

4. Alignment using the magnetic axis of the main coil only (which should be the same as the geometric axis, assuming the main coil is ideal) gives better results for beam trajectories than using the average zero flux magnetic axis (e.g. as determined by stretched wire) for the cases considered.

5. The magnitude of trajectory errors caused by the optical properties of a non-ideal lens are comparable to those of an ideal lens which is misaligned (at the present values of tolerances).

6. Beam-based alignment can be considered if better than 0.3 mm positioning accuracy is needed.

References:

1] B. Mustapha, et al., "Misalignment Error and Alignment Specs", http://tdweb.fnal.gov/HINS/MeetingMinutes/2006/20061116/
2] J. DiMarco, et al., “Solenoid Magnet Alignment at Fermilab”, IMMW-16, Oct 2009, http://immw16.web.psi.ch/Presentations/2_16_IMMW16_Fiducialization.pdf
3] M. Reiser, et al., “Study of Misalignment Effects in Electron Beam Transport through a Periodic Solenoid Channel”, PAC‘87 Proceedings, pp. 1135 – 1137.
4] T. M. Page, et al., “HINS Superconducting Lens and Cryostat Performance,” *Trans. Appl. Supercon.*, vol. 19, no. 3, June 1009, pp. 1356-1359.
5] M. Tartaglia, et al., “Summary of HINS Focusing Solenoid Production and Test”, MT-21, China, Oct. 2009, FERMILAB-CONF-09-143-TD.
6] I. Terechkine, “Short Solenoid Focusing Channel for PD Front End”, TD-05-035
7] “Handbook of Accelerator Physics and Engineering”, ed. W. Chao and M. Tigner, World Scientific, 1999, p. 59.
8] http://en.wikipedia.org/wiki/Aberration_in_optical_systems
9] T. Schmidt, et al., “The Pulsed Wire Magnetic Measurement System”, IMMW-16, Oct., 2009, http://immw16.web.psi.ch/Presentations/2_15_IMMW16_Fiducialization.pdf